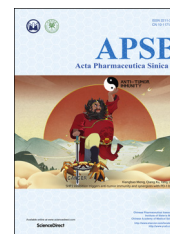




Chinese Pharmaceutical Association  
Institute of Materia Medica, Chinese Academy of Medical Sciences

Acta Pharmaceutica Sinica B

[www.elsevier.com/locate/apsb](http://www.elsevier.com/locate/apsb)  
[www.sciencedirect.com](http://www.sciencedirect.com)



ORIGINAL ARTICLE

# Biosynthesis of clinically used antibiotic fusidic acid and identification of two short-chain dehydrogenase/reductases with converse stereoselectivity



Zhiqin Cao<sup>a,†</sup>, Shaoyang Li<sup>a,†</sup>, Jianming Lv<sup>a,†</sup>, Hao Gao<sup>a</sup>,  
Guodong Chen<sup>a</sup>, Takayoshi Awakawa<sup>b</sup>, Ikuro Abe<sup>b</sup>, Xinsheng Yao<sup>a,\*</sup>,  
Dan Hu<sup>a,\*</sup>

<sup>a</sup>Institute of Traditional Chinese Medicine and Natural Products, College of Pharmacy/Guangdong Province Key Laboratory of Pharmacodynamic Constituents of TCM and New Drugs Research, Jinan University, Guangzhou 510632, China

<sup>b</sup>Graduate School of Pharmaceutical Sciences, The University of Tokyo, 7-3-1 Hongo, Bunkyo-ku, Tokyo 113-0033, Japan

Received 17 August 2018; received in revised form 17 October 2018; accepted 25 October 2018

## KEY WORDS

Biosynthesis;  
Fungi;  
Fusidic acid;  
Fusidane-type antibiotics;  
SDR

**Abstract** Fusidic acid is the only fusidane-type antibiotic that has been clinically used. However, biosynthesis of this important molecule in fungi is poorly understood. We have recently elucidated the biosynthesis of fusidane-type antibiotic helvolic acid, which provides us with clues to identify a possible gene cluster for fusidic acid (*fus* cluster). This gene cluster consists of eight genes, among which six are conserved in the helvolic acid gene cluster except *fusC1* and *fusB1*. Introduction of the two genes into the *Aspergillus oryzae* NSAR1 expressing the conserved six genes led to the production of fusidic acid. A stepwise introduction of *fusC1* and *fusB1* revealed that the two genes worked independently without a strict reaction order. Notably, we identified two short-chain dehydrogenase/reductase genes *fusC1* and *fusC2* in the *fus* cluster, which showed converse stereoselectivity in 3-ketoreduction. This is the first report on the biosynthesis and heterologous expression of fusidic acid.

© 2019 Chinese Pharmaceutical Association and Institute of Materia Medica, Chinese Academy of Medical Sciences. Production and hosting by Elsevier B.V. This is an open access article under the CC BY-NC-ND license (<http://creativecommons.org/licenses/by-nc-nd/4.0/>).

\*Corresponding authors.

E-mail addresses: [tyaoxs@jnu.edu.cn](mailto:tyaoxs@jnu.edu.cn) (Xinsheng Yao), [thudan@jnu.edu.cn](mailto:thudan@jnu.edu.cn) (Dan Hu).

<sup>†</sup>These authors made equal contributions to this work.

Peer review under responsibility of Institute of Materia Medica, Chinese Academy of Medical Sciences and Chinese Pharmaceutical Association.

<https://doi.org/10.1016/j.apsb.2018.10.007>

2211-3835 © 2019 Chinese Pharmaceutical Association and Institute of Materia Medica, Chinese Academy of Medical Sciences. Production and hosting by Elsevier B.V. This is an open access article under the CC BY-NC-ND license (<http://creativecommons.org/licenses/by-nc-nd/4.0/>).

## 1. Introduction

Fusidane-type antibiotics belong to a small group of fungi-derived 29-*nor* protostane triterpenoids, which are represented by fusidic acid (**1**), helvolic acid and cephalosporin P<sub>1</sub> (Fig. 1A)<sup>1</sup>. They exhibit potent bacteriostatic activity against Gram-positive bacteria, and among them fusidic acid has been clinically used since 1962 for the treatment of both topical and systemic infections caused by *Staphylococcus aureus*<sup>2,3</sup>. As fusidane-type antibiotics are the only known antibiotics that target elongation factor EF-G to inhibit bacterial protein synthesis<sup>4,5</sup>, they have no cross-resistance with commonly used antibiotics, which have drawn much attention in the increasing threat of antimicrobial resistance<sup>6</sup>. Fusidane-type antibiotics have been subjected to extensive chemical synthesis and derivatization<sup>7–10</sup>, however, more potent analogues than fusidic acid have not been found thus far. Combinational biosynthesis is an alternative approach to generate chemical diversity, which however requires a deep understanding of the biosynthesis of target compounds.

Previous studies on the biosynthesis of fusidane-type antibiotics are mainly dependent on the feeding experiments using isotopically labeled precursors<sup>11</sup>. However, the genetic basis for the biosynthesis of fusidane-type antibiotics remains elusive until 2009 when a cluster for helvolic acid was identified from the genome of *A. fumigatus* Af293<sup>12,13</sup>. This gene cluster consists of nine genes, among which HelA (oxidosqualene cyclase, OSC) was revealed to catalyze the cyclization of 2,3(*S*)-oxidosqualene to form the carbon skeleton protostadienol, and HelC (short-chain dehydrogenase/reductase, SDR) and HelB1 (cytochrome P450, P450) were shown to be responsible for the conversion of protostadienol to its 3-keto and 4 $\beta$ -carboxylic acid derivatives, respectively<sup>13</sup>. To shed light on the whole biosynthetic pathway for helvolic acid, we have recently reconstituted all the nine genes in a step wise manner in a quadruple auxotrophic *A. oryzae* NSAR1<sup>14</sup>, which allows us to elucidate the complete biosynthetic pathway for helvolic acid and the functions of the rest six genes<sup>15</sup>. Despite these, biosynthesis of the clinically used fusidic acid remains elusive.

In the present study, we first sequenced the genome of the fusidic acid producer *Acremonium fusidioides* ATCC 14700 and identified a possible gene cluster by searching for the HelA homologue. This gene cluster consists of eight genes, among which six are conserved in helvolic acid gene cluster. Reconstitution of these genes in *A. oryzae* NSAR1 has led to the production of fusidic acid and characterization of its full biosynthetic pathway. This study has provided a basis for expanding chemical diversity of fusidane-type antibiotics using biosynthetic approaches.

## 2. Materials and methods

### 2.1. General materials and experimental procedures

Acetonitrile (MeCN) was purchased from Oceanpak Alexative Chemical Co., Ltd. (Gothenburg, Sweden). Ethyl acetate (EtOAc) and acetone were analytical grade from Fine Chemical Co., Ltd. (Tianjin, China). Formic acid was obtained from Kemiou Chemical Reagent Co., Ltd. (Tianjin, China).

Primer synthesis and DNA sequencing were performed by Sangon Biotech Co., Ltd. (Shanghai, China). Plasmid extraction kits and DNA purification kits were purchased from Sangon

Biotech Co., Ltd. (Shanghai, China). PCR was performed using KOD-FX DNA polymerase or KOD-Plus DNA polymerase (Toyobo, Osaka, Japan). In-Fusion<sup>®</sup> HD Cloning Kit or T4 DNA ligase were purchased from Takara Bio Inc. (Dalian, China). DNA restriction enzyme were purchased from Thermo Fisher Scientific (Shenzhen, China).

The HR-ESI-MS spectra were obtained with a Waters Synapt G2 TOF mass spectrometer (Waters Corporation, Milford, USA). The 1D and 2D NMR spectra were acquired with Bruker AV 400 or Bruker AV 600 spectrometers (Bruker BioSpin Group, Faelanden, Switzerland) using the solvent signals (CDCl<sub>3</sub>:  $\delta_{\text{H}}$  7.26/ $\delta_{\text{C}}$  77.0) as internal standards.

High-performance liquid chromatography (HPLC) and liquid chromatography–mass spectrometry (LC–MS) were carried out on an Ultimate 3000 HPLC system (Dionex) and an amaZon SL ion trap mass spectrometer (Bruker) using electrospray ionization with a YMC-pack ODS-A column (250 mm  $\times$  4.6 mm i.d., 5  $\mu$ m; YMC Co., Ltd., Japan). Elution was subjected to a linear gradient [H<sub>2</sub>O containing 0.1% formic acid (A) and CH<sub>3</sub>CN containing 0.1% formic acid (B); 1 mL/min; 50%–100% B (0–30 min), 100% B (10 min); 208 nm].

The semi-preparative HPLC was carried out on an Ultimate 3000 HPLC system (Dionex) equipped with UV detector, using a YMC-Pack ODS-A column (250 mm  $\times$  10.0 mm i.d., 5  $\mu$ m) (YMC Co., Ltd., Kyoto, Japan). Medium pressure liquid chromatography (MPLC) was carried out on a UV preparative detector, a dual pump gradient system, and a Dr. Flash II fraction collector system (Lisui E-Tech Co., Ltd., Shanghai, China). Column chromatography (CC) was performed with ODS (50  $\mu$ m, YMC Co., Ltd., Tokyo, Japan).

### 2.2. Strains and media

*A. fusidioides* ATCC 14700 was obtained from the American Type Culture Collection (Maryland, USA). *A. fusidioides* ATCC 14700 was cultivated at 28 °C, 150 rpm (IS-RDS4 incubator, Crystal Technology & Industries, Inc., Beijing, China) in PDB medium for 3 days, and served as a source for whole genome sequencing and the cloning of the *fusC1*, *fusB1* and *fusC2* genes.

*Aspergillus oryzae* NSAR1 (*sC*<sup>-</sup>, *niaD*<sup>-</sup>,  *$\Delta$ argB*, *adeA*<sup>-</sup>) was used as the host for heterologous expression<sup>14</sup>. Transformants of *A. oryzae* NSAR1 were cultured in the 50 mL centrifuge tube with 15 mL DPY medium (2% dextrin, 1% polypeptone, 0.5% yeast extract, 0.05% MgSO<sub>4</sub>·7H<sub>2</sub>O, 0.5% KH<sub>2</sub>PO<sub>4</sub>) for 2 days at 28 °C and 150 rpm as seed broth. The cells were then transferred into Czapek–Dox (CD) medium with polypepton and starch (0.3% NaNO<sub>3</sub>, 0.2% KCl, 0.05% MgSO<sub>4</sub>·7H<sub>2</sub>O, 0.1% KH<sub>2</sub>PO<sub>4</sub>, 0.002% FeSO<sub>4</sub>·7H<sub>2</sub>O, 1% polypeptone, 2% starch, pH 5.5) to induce gene expression under the *amyB* promoter, and cultured for 5 to 6 days.

Standard DNA engineering experiments were performed using *E. coli* DH5 $\alpha$ . *E. coli* cells bearing each plasmid were grown in Luria–Bertani (LB) medium with appropriate antibiotics, and *E. coli* BL21-Codon Plus (DE3) was used for recombinant expression of FusC1 and FusC2 (Supporting Information Fig. S1).

### 2.3. Whole genome sequencing and analysis

Genome sequencing of *A. fusidioides* ATCC 14700 was performed by Sangon Biotech Co., Ltd. (Shanghai, China) with an Illumina HiSeq. 2500 system. Sequence assembly was

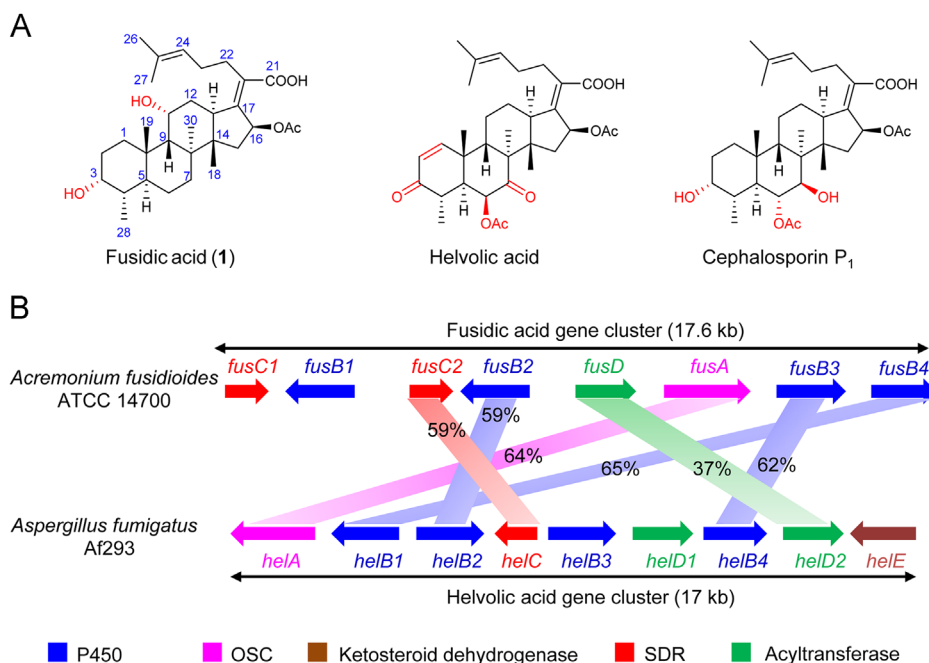


**Figure 1** Representative fusidane-type antibiotics and gene cluster comparison between fusidic acid and helvolic acid. (A) Chemical structures of three representative fusidane-type antibiotics: fusidic acid (1), helvolic acid and cephalosporin P<sub>1</sub>. (B) Schematic representation of the gene clusters of fusidic acid and helvolic acid, and their amino acid sequence identities.

performed with SOAPdenovo version 2.04 (<http://soap.genomics.org.cn/soapdenovo.html>) to yield 662 contigs covering approximately 31.9 Mb. The contig N50 length is approximately 112,188. Gene functional annotation was based on blast searches of KOG, TrEMBL, Swissprot, GO, KEGG, PFAM, NR and CDD databases, and manually revised by comparisons with homologous genes in the NCBI database (<https://www.ncbi.nlm.nih.gov/>). All the predicted genes were used to construct a protein database for local BLAST search.

#### 2.4. Phylogenetic analysis

The full-length protein sequences of all related enzyme were collected from GenBank and JGI database, and aligned using ClustalW. A rooted maximum likelihood tree was generated using poisson model by MEGA 6.0 software with bootstrapping for 1000 replicates.

#### 2.5. Construction of fungal expression plasmids

To construct the fungal expression plasmids for the *fusC1* and *fusB1* genes. *fusC1* and *fusB1* were initially amplified from *A. fusidoides* ATCC 14700 genomic DNA and cDNA, respectively. The primers used for the amplification are listed in Supporting Information Table S1. The full-length genes were purified, digested with *EcoRI* and *KpnI*, and ligated into the pTAex3 vector using the T4 DNA ligase (TaKaRa), to afford pTAex3-*fusC1* and pTAex3-*fusB1*.

pPTRI-*fusC1* and pPTRI-*fusB1* were respectively constructed by the insertion of fragments amplified from pTAex3-*fusC1*, and pTAex3-*fusB1* with the primers pPTRI-Pamy-F/pPTRI-Tamy-R into the *HindIII*-digested pPTRI vector using the In-Fusion<sup>®</sup> HD Cloning Kit. For construction of plasmid harboring the two genes, the two fragments amplified from pTAex3-*fusC1* and pTAex3-*fusB1*,

respectively, were ligated into the *HindIII*-digested pPTRI using the In-Fusion<sup>®</sup> HD Cloning Kit. All of the expression plasmids are listed in Supporting Information Table S2.

#### 2.6. Transformation of *A. oryzae* NSAR1

Transformation of *A. oryzae* NSAR1 was performed as previously described<sup>16</sup>. The spore suspension of *A. oryzae* NSAR1 was inoculated into 10 mL DPY medium and cultivated at 28 °C and 150 rpm for 2 days. The cells were then transferred into 100 mL DPY medium and grown for 1 day at 28 °C and 150 rpm. Mycelia were collected by filtration and digested with 1% Yatalase (Takara) in 0.6 mol/L (NH<sub>4</sub>)<sub>2</sub>SO<sub>4</sub>, 50 mmol/L maleic acid, pH 5.5 at 30 °C for 3 h. After removing residues by filtration, protoplasts were centrifuged at 1500 rpm for 10 min and washed with Solution 2 (1.2 mol/L sorbitol, 35 mmol/L NaCl, 50 mmol/L CaCl<sub>2</sub>·2H<sub>2</sub>O, 10 mmol/L Tris-HCl, pH 7.5), and then adjusted to 2 × 10<sup>7</sup> cells/mL in Solution 2. A mixture of 200 μL protoplasts solution and 10 μg plasmids was incubated on ice for 30 min, and subsequently a total of 1.35 mL (250, 250, and 850 μL) Solution 3 (60% PEG4000, 50 mmol/L CaCl<sub>2</sub>·2H<sub>2</sub>O, 10 mmol/L Tris-HCl, pH 7.5) was added to the aliquot. After incubating for 20 min at the room temperature, 10 mL Solution 2 was added, and then the mixture was centrifuged at 1500 rpm for 10 min. The precipitates were suspended in 200 μL Solution 2 and spread on the lower selective medium (0.1% (NH<sub>4</sub>)<sub>2</sub>SO<sub>4</sub>, 0.2% NH<sub>4</sub>Cl, 0.05% NaCl, 0.05% KCl, 0.1% KH<sub>2</sub>PO<sub>4</sub>, 0.05% MgSO<sub>4</sub>·7H<sub>2</sub>O, 0.002% FeSO<sub>4</sub>·7H<sub>2</sub>O, 2% glucose and 1.2 mol/L sorbitol as well as 0.15% methionine, 0.1% arginine, 0.01% adenine, and 0.1 μg/mL pyrithiamine hydrobromide if necessary, pH 5.5) with 1.5% agar, and then covered with the selective upper medium containing 0.8% agar. The plates were incubated at 30 °C for 5–7 days. The six-gene expression strain<sup>15</sup> was transformed with pPTRI-*fusC1*-*fusB1*, pPTRI-*fusB1* or pPTRI-*fusC1*.

### 2.7. Isolation and purification of metabolites

For the analysis of the metabolites in different transformants, the culture medium was extracted with EtOAc and mycelia were extracted with acetone at room temperature overnight. The extract was concentrated under reduced pressure, and resuspended for analysis. For isolation of metabolites, the culture medium extract was subjected to the ODS column chromatography and further purification by semi-preparative HPLC (Supporting Information Methods).

### 2.8. Recombinant expression and purification of FusC1 and FusC2

The cDNA fragments encoding FusC1 and FusC2 were amplified from *A. fusidioides* ATCC14700 genomic DNA with the primers listed in Supporting Information Table S1, and ligated into the pET-28a(+) vector digested with *Nde*I using the In-Fusion<sup>®</sup> HD Cloning Kit, respectively.

For the expression of *fusC1* and *fusC2*, *fusC1* or *fusC2* with an *N*-terminal His<sub>6</sub>-tag was expressed in *E. coli* BL21-Codon Plus (DE3). The cells were cultured at 37 °C, 200 rpm overnight in 10 mL of LB medium with 50 mg/L kanamycin and then 1.5 mL seed broth was transferred into the 500 mL flask with 150 mL LB medium and 50 mg/L kanamycin, and grew at 37 °C and 200 rpm. Gene expression was induced by the addition of 0.2–0.3 mmol/L isopropyl  $\beta$ -D-1-thiogalactopyranoside (IPTG) when the cultures had grown to OD<sub>600</sub> of 0.5–0.7. The cells were further cultured at 18 °C for 12–16 h before harvested by centrifugation at 4 °C and 5000  $\times$  *g* for 15 min. The cells pellets were resuspended in lysis buffer (50 mmol/L Tris-HCl, 200 mmol/L NaCl, 5 mmol/L imidazole, 5% glycerol, pH 8.0), and lysed by sonication on ice. The His<sub>6</sub>-tagged proteins were purified by using Ni-NTA affinity column (GE Healthcare Bio-Sciences AB, Uppsala, Sweden) according to previously reported methods<sup>15</sup>. The purified enzyme was analyzed by sodium dodecyl sulfate polyacrylamide gel electrophoresis (SDS-PAGE). Protein concentration was quantified according to the Bradford method by Pierce<sup>™</sup> BCA Protein Assay Kit (Thermo Fisher Scientific Inc., Rockford, USA).

### 2.9. Enzymatic reaction assay of FusC1, FusC2, and HelC

The enzymatic assays of FusC1, FusC2, and HelC were performed in a 200  $\mu$ L reaction mixture containing 100 mmol/L Tris-HCl (pH 7.0), 5 mmol/L NADH or NADPH, 2.35–7.00  $\mu$ mol/L enzymes, and 0.5 mmol/L substrate as previously described<sup>15</sup>. The reactions with inactivated enzymes were used as negative controls. Each reaction was incubated at 30 °C for 12 h and extracted twice with 200  $\mu$ L ethyl acetate. The solvents were dried and dissolved in 50  $\mu$ L of MeOH and subjected to HPLC analysis. Integrated peak areas for the substrate and product were used to calculate the conversion efficiency and normalized to the activity of enzymes in standard condition.

### 2.10. Determination of the kinetics parameters of FusC1 and FusC2

100  $\mu$ L reactions contained 100 mmol/L Tris-HCl (pH 7.0), 500  $\mu$ mol/L cofactor (NADPH or NADH), 0.2  $\mu$ mol/L enzyme (FusC1 or FusC2), and 5  $\mu$ mol/L to 600  $\mu$ mol/L **2** in DMSO. After a preincubation at 30 °C for 3 min, the reactions were initiated by

adding the substrates, and continued for 2.5 min. Among them, the reaction of FusC2 in the presence of NADPH was carried out for 25 min. All the reactions were terminated by adding 100  $\mu$ L methanol and mixed by vortex. After centrifugation, the supernatant was analyzed by HPLC and quantified by a standard curve. Assays were conducted in duplicate, and all rates were confirmed to be linear. The kinetics curves were fit to the Michaelis–Menten equation using GraphPad Prism 6 (GraphPad Software, La Jolla, CA, USA).

### 2.11. Feeding experiments

Transformant harboring pTAex3-*fusB1* plasmid was inoculated to 10 mL DPY medium for 2–3 days, and then inoculated into 50 mL CD medium for inducing the expression of *fusB1*. After cultivation for 24 h, the culture medium was supplemented with 1.0 mg of **5** dissolved in 30  $\mu$ L DMSO and was cultivated for another 3 days. The culture medium was extracted with an equal volume of EtOAc and the dried extract was dissolved in MeOH for HPLC analysis.

### 2.12. Antibacterial assay

Antibacterial activity of compounds **1**, **3**, **4**, and **5** against Gram-positive strain *Staphylococcus aureus* 209 P was evaluated using the 2-fold dilution assay<sup>17–19</sup>. Seed cultures of *S. aureus* 209 P was inoculated on beef extract medium at 37 °C for 1 day. The resulting seed culture were collected with normal saline and adjusted to a concentration of 10<sup>7</sup>–10<sup>9</sup> mL, and then added to each well of 96-well microtiter plates (100  $\mu$ L/well). These bacteria were treated with a serial 2-fold dilution of each compound, ranging from 128 to 0.002  $\mu$ g/mL. Tobramycin was used as the positive control and DMSO was used as the negative control. The 96-well microtiter plates were placed in an incubator at 37 °C for 24 h. The MICs were defined as the minimal concentration at which no growth of bacteria could be observed.

### 2.13. Structural characterization

Compound **1**: a white powder; HR-ESI-MS (positive) *m/z* 517.3539 [M + H]<sup>+</sup> (Calcd. for C<sub>31</sub>H<sub>49</sub>O<sub>6</sub>, 517.3529), see Supporting Information Fig. S7A; NMR spectra, see Supporting Information Fig. S7B–C; NMR data, see Supporting Information Table S4; The NMR data are in good agreement with those of fusidic acid<sup>20</sup> (Supporting Information Note 1).

Compound **3**: a yellowish powder; HR-ESI-MS (positive) *m/z* 515.3395 [M + H]<sup>+</sup> (Calcd. for C<sub>31</sub>H<sub>47</sub>O<sub>6</sub>, 515.3373), see Supporting Information Fig. S8A; NMR spectra, see Supporting Information Fig. S8B–G; NMR data, see Supporting Information Table S5; the structure is as the same as that of 3-oxofusidic acid<sup>21</sup>, the detailed NMR assignments of which are not available prior to the present study (Supporting Information Note 2).

Compound **4**: a yellowish powder; HR-ESI-MS (positive) *m/z* 517.3496 [M + H]<sup>+</sup> (Calcd. for C<sub>31</sub>H<sub>49</sub>O<sub>6</sub>, 517.3529), see Supporting Information Fig. S9A; NMR spectra, see Supporting Information Fig. S9B–G; NMR data, see Supporting Information Table S6; the structure is as the same as that of 3-epifusidic acid<sup>21</sup>, the detailed NMR assignments of which are not available prior to the present study (Supporting Information Note 3).

Compound **5**: a white powder; HR-ESI-MS (positive) *m/z* 501.3570 [M + H]<sup>+</sup> (Calcd. for C<sub>31</sub>H<sub>49</sub>O<sub>5</sub>, 501.3580), see Supporting

Information Fig. S10A; NMR spectra, see Supporting Information Fig. S10B–G; NMR data, see Supporting Information Table S7; the structure is as the same as that of 11-deoxyfusidic acid<sup>22</sup>, the detailed NMR assignments of which are not available prior to the present study (Supporting Information Note 4).

### 3. Results

#### 3.1. Identification of the biosynthetic gene cluster for fusidic acid

To reveal the molecular basis for the biosynthesis of fusidic acid, we purchased its producer *A. fusidioides* ATCC 14700 from the American Type Culture Collection (ATCC). Production of fusidic acid by this strain was confirmed by comparison with the authentic compound via LC–MS analysis (Supporting Information Fig. S2). We then sequenced the whole genome of *A. fusidioides* and identified a possible gene cluster for fusidic acid by searching of the *HelA* homologue (Fig. 1B). This gene cluster (designated as *fus* cluster, accession number: MK044769) consists of eight genes, encoding one oxidosqualene cyclase (*fusA*), four cytochrome P450s (*fusB1–B4*), one acyltransferase (*fusD*), two short-chain dehydrogenase/reductases (*fusC1–C2*) (Fig. 1B and Table 1). Among them, six genes, *fusA*, *fusB2*, *fusB3*, *fusB4*, *fusC2* and *fusD* encode proteins with high sequence similarity (37%–65% identity) to those encoded by *helA*, *helB2*, *helB4*, *helB1*, *helC* and *helD2* in the gene cluster of helvolic acid. Coincidentally, we have previously shown that the six genes are involved in the early-stage biosynthesis of helvolic acid<sup>15</sup>. Based on these facts, we hypothesized that the six-gene-mediated reaction is likely to be a common pathway in the early stage biosynthesis of all fusidane-type antibiotics to give the key intermediate **2**, which is then bifurcated to generate different fusidane-type antibiotics under the action of different post-modification enzymes (Fig. 2D). A similar phenomenon has also been found in the biosynthesis of citreohydrinol and paraherquonin<sup>23,24</sup>.

To test this hypothesis, we introduced the two uncharacterized genes *fusC1* and *fusB1* into the six-gene expression strain established in our previous study by co-expression of *helA*, *helB2*, *helB4*, *helB1*, *helC* and *helD2*. The transformant was cultured in an induction medium for 6 days, and the supernatant extract was analyzed by HPLC. As shown in Fig. 2A(v), compared to the six-gene expression strain (Fig. 2A(ii)) that dominantly produced **2**, introduction of *fusC1* and *fusB1* led to the generation of an additional compound **1**. This compound was isolated and structurally determined to be fusidic acid. The yield of fusidic acid in the heterologous expression of *A. oryzae* is around 14.3 mg/L, which is much higher than that of the wild-type strain *A. fusidioides* ATCC 14700. Therefore, using a combinational biosynthetic

approach, we have identified the gene cluster for fusidic acid and achieved its heterologous expression.

#### 3.2. Characterization of the biosynthetic pathway for fusidic acid

To address whether FusB1 and FusC1 can only function after the action of the conserved six genes, we introduced *fusC1* and *fusB1* into the *helC*-lacked five-gene expression strain (*helA*, *B1*, *B2*, *B4*, and *D2*) because we have shown that HelC catalyzes the final step in the six-gene mediated reaction<sup>15</sup>. As shown in Supporting Information Fig. S3, no additional peaks were observed, suggesting that FusC1 and FusB1 can only function after the conserved six genes.

We then carried out the stepwise introduction of *fusC1* and *fusB1* to the six-gene expression strain for elucidating the full biosynthetic pathway of fusidic acid. As shown in Fig. 2A(iii), introduction of *fusB1* to the six-gene expression strain gave two additional compounds **3** and **4**. NMR structural characterization showed that **3** was featured with an  $\alpha$ -hydroxyl group at the C-11 compared to **2**, indicating that FusB1 (P450) was responsible for  $\alpha$ -hydroxylation of C-11 (Fig. 2D). And the minor product **4** was elucidated as the 3-keto reduced product of **3**. On the other hand, addition of *fusC1* also led to the appearance of a new peak **5** (Fig. 2A(iv)). Isolation and structural determination of **5** indicated that it contains a 3 $\alpha$ -hydroxyl group, suggesting that FusC1 catalyzes the specific reduction of 3-keto to 3 $\alpha$ -OH (Fig. 2D).

The above results clearly showed that both FusB1 and FusC1 could accept **2** as a substrate to generate **3** and **5**, respectively, but it is still not clear whether **1** is formed from **3** by FusC1 or from **5** under the action of FusB1. To address these issues, FusC1 was expressed in *E. coli* BL21-Codon Plus (DE3) (Supporting Information Fig. S1), purified and incubated with **3**. An efficient conversion of **3** to **1** by FusC1 was observed (Fig. 2B(iv)), but not the denatured FusC1 (Fig. 2B(iii)). Since FusB1 is a membrane-type P450 enzyme and difficult to be actively expressed in *E. coli*, feeding experiment was carried out by establishing a transformant strain harboring only *fusB1*. As shown in Fig. 2C, we observed that *fusB1*-harboring strain but not the control strain could generate **1** when supplemented with **5**. These results clearly indicated that fusidic acid can be generated from both **3** and **5** by FusC1 and FusB1, respectively (Fig. 2D).

#### 3.3. Identification of two SDR enzymes with converse stereoselectivity in the *fus* cluster

In this study as well as our previous study on the biosynthesis of helvolic acid, we often observed the co-existence of 3 $\beta$ -OH derivatives with their corresponding 3-keto derivatives (Fig. 2A

**Table 1** Putative functions of genes in the fusidic acid gene cluster.

Gene	Protein homologue, origin	Similarity/identity (%)	Proposed function
<i>fusC1</i>	MGYG_08624, <i>Nannizzia gypsea</i> CBS 118893	78/63	Short-chain dehydrogenase/reductasereductase
<i>fusB1</i>	MGYG_08623, <i>Nannizzia gypsea</i> CBS 118893	86/78	Cytochrome P450
<i>fusC2</i>	HelC, <i>Aspergillus fumigatus</i> Af293	72/59	Short-chain dehydrogenase/reductase
<i>fusB2</i>	HelB2, <i>Aspergillus fumigatus</i> Af293	75/59	Cytochrome P450
<i>fusD</i>	HelD2, <i>Aspergillus fumigatus</i> Af293	53/37	Acyltransferase
<i>fusA</i>	HelA, <i>Aspergillus fumigatus</i> Af293	77/64	Oxidossqualene cyclase
<i>fusB3</i>	HelB4, <i>Aspergillus fumigatus</i> Af293	78/62	Cytochrome P450
<i>fusB4</i>	HelB1, <i>Aspergillus fumigatus</i> Af293	79/65	Cytochrome P450

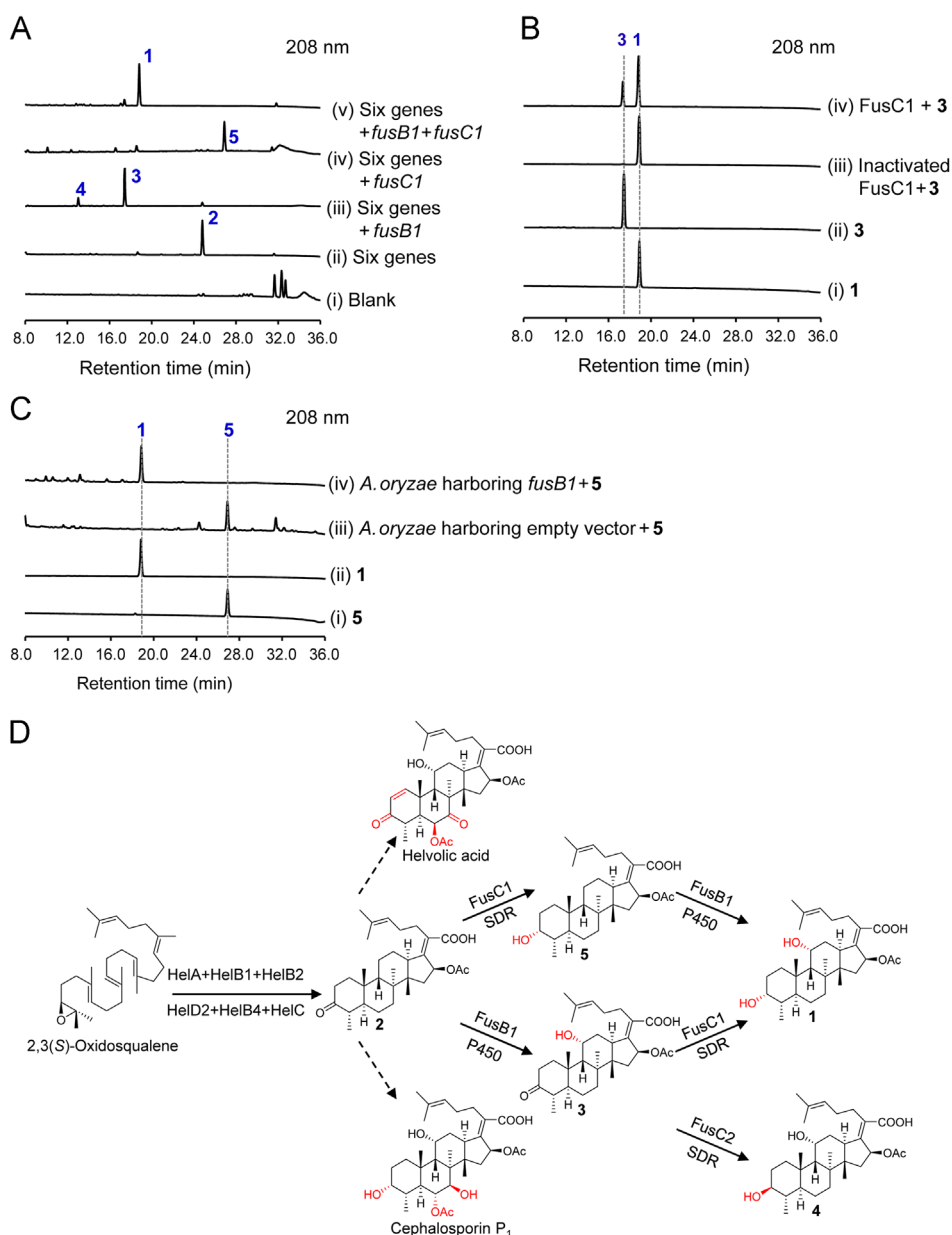


**Figure 2** Biosynthesis of fusidic acid. (A) HPLC analysis of culture supernatant extract from various *A. oryzae* transformants: (i) Blank medium; (ii) *A. oryzae* transformant expressing the conserved six genes (*hela*, *B1*, *B2*, *C*, *B4*, and *D2*); (iii) *A. oryzae* transformant expressing the conserved six genes and *fusB1*; (iv) *A. oryzae* transformant expressing the conserved six genes and *fusC1*; (v) *A. oryzae* transformant expressing the conserved six genes, *fusB1* and *fusC1*. (B) HPLC analysis of *in vitro* enzymatic reaction with FusC1: (i) compound 1; (ii) compound 3; (iii) compound 3 with inactivated FusC1; (iv) compound 3 with FusC1. (C) HPLC analysis of culture supernatant extract of *A. oryzae* harboring *fusB1* fed with 5: (i) compound 5; (ii) compound 1; (iii) *A. oryzae* harboring the empty vector incubated with 5; (iv) *A. oryzae* harboring *fusB1* incubated with 5. (D) Schematic representation of the biosynthetic pathway of fusidic acid.

(iii)), but the enzyme for the specific conversion of 3-keto to 3 $\beta$ -OH remains elusive. Among the conserved six genes, there is a gene encoding a short-chain dehydrogenase/reductase (HelC), responsible for the dehydrogenation of 3 $\beta$ -OH to 3-keto in the presence of NAD<sup>+</sup>. Since some SDR enzymes are able to catalyze the reversible reduction/dehydrogenation<sup>25</sup>, we wondered whether this conserved SDR enzyme (HelC) accounts for the formation of 3 $\beta$ -OH derivatives. We then incubated HelC with 3 in the presence of NADH. As expected, we observed an efficient conversion of 3 to 4 by HelC (Supporting Information Fig. S4B). We then cloned *fusC2* (homologue of *helC*) from the *fus* cluster and expressed it in

*E. coli* BL21-Codon Plus (DE3) (Supporting Information Fig. S1). *In vitro* enzymatic assay of FusC2 along with FusC1 was carried out using the same substrate 2 (Fig. 3). Both FusC1 and FusC2 could accept 2 as a substrate. FusC1 specifically converted 3-keto to 3 $\alpha$ -OH (Fig. 3A), while FusC2 catalyzed the specific reduction of 3-keto to 3 $\beta$ -OH (Fig. 3B). These results indicated that FusC2 and HelC were responsible for the formation of 3 $\beta$ -OH derivatives during the biosynthesis of fusidic acid and helvolic acid. In addition, we also demonstrated that the 3 $\beta$ -OH-containing products 6, 8 and 10 during helvolic acid biosynthesis were generated from 2, 7, and 9 by HelC (Supporting Information Fig. S4).

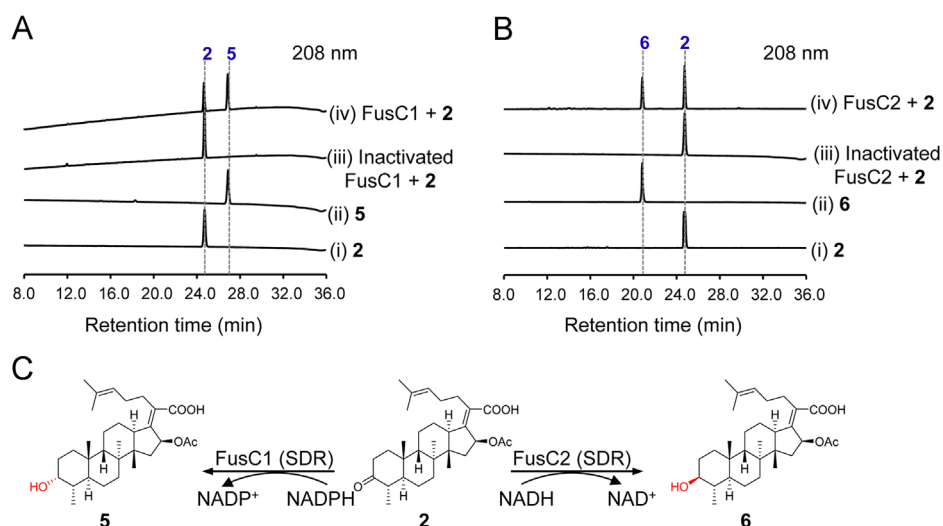


**Figure 3** *In vitro* enzymatic assay of FusC1 and FusC2. (A) HPLC analysis of *in vitro* enzymatic reaction with FusC1: (i) compound **2**; (ii) compound **5**; (iii) **2** with inactivated FusC1; (iv) **2** with FusC1. (B) HPLC analysis of *in vitro* enzymatic reaction with FusC2: (i) compound **2**; (ii) compound **6**; (iii) **2** with inactivated FusC2; (iv) **2** with FusC2. (C) Schematic representation of stereoselective reduction of 3-keto by FusC1 and FusC2.

The above results showed that the 3β-OH derivatives were formed by the conserved SDR enzymes FusC2 or HelC, but they were always produced as minor products (Fig. 2A(iii)). Especially in the presence of FusC1, 3β-OH derivatives were hardly detected. These results drive us to compare the catalytic efficiency of FusC1 and FusC2 at 30 °C, a standard temperature of the incubation of fungi. We first determined the optimal pH for both enzymes and found that both of them preferred pH 7.0 (Fig. 4A and B). We then compared the catalytic efficiency of FusC1 and FusC2 in the presence of NADPH or NADH by monitoring the conversion rate over time. As shown in Fig. 4C and D, in the presence of NADPH, FusC1-mediated reduction was more efficient than FusC2, but FusC2 catalyzed more efficiently in the presence of NADH. These results suggested that the co-factors may function to regulate the production of 3β-OH and 3α-OH derivatives.

To further characterize the enzymatic properties of FusC1 and FusC2, we measured their steady-state kinetic parameters using **2** as a substrate. In the presence of NADH, the  $K_m$  value of FusC1 is 38.77 μmol/L, which is only slightly higher than that of FusC2 (32.80 μmol/L), while the  $K_{cat}/K_m$  value of FusC1 (0.89 L/min/μmol) is much lower than that of FusC2 (2.24 L/min/μmol) (Fig. 5A and B and Table 2). This result is consistent with the fact that FusC1 is less efficient than FusC2 in the presence of NADH (Fig. 4D). On the other hand, in the presence of NADPH, the  $K_m$  value of FusC1 is 70.03 μmol/L, which is lower than that of FusC2 (151.20 μmol/L), and the  $K_{cat}/K_m$  value of FusC1 (3.89 L/min/μmol) is 200-fold higher than that of FusC2 (0.02 L/min/μmol) (Fig. 5C and D and Table 2), indicating a greater substrate affinity and significantly higher catalytic efficiency of FusC1 in the presence of NADPH. These results are highly consistent with the results that FusC1 is much efficient than FusC2 in the presence of NADPH (Fig. 4C).

### 3.4. Structure–activity analysis of fusidic acid derivatives

In the course of our work, we obtained fusidic acid and its 3 analogues *via* heterologous expression in *A. oryzae*. Their inhibitory effects against *S. aureus* 209 P was carried out by the 2-fold dilution method using tobramycin as a positive control. As

shown in Table 3, all the compounds exhibited potent bacteria-killing activity. Among them, fusidic acid (**1**) showed the most potent antibacterial activity with an MIC value of 0.004 μg/mL, which was stronger than that of **3** (MIC = 0.25 μg/mL) and **4** (MIC = 8 μg/mL), suggesting that 3α-OH was more important than 3-keto and 3β-OH. Comparison of **1** and **5** also indicated that the 11α-OH was critical for the activity, which was consistent with previous reports<sup>7</sup>.

## 4. Discussion

Fusidic acid is a fungi-derived triterpenoid antibiotic and has been clinically used since 1960s for the treatment of infections caused by Gram-positive bacteria. Here, we reported the identification of the biosynthetic gene cluster of fusidic acid and its heterologous expression in *A. oryzae* using a combinational strategy. Notably, we identified two SDR enzymes with opposite stereoselectivity from the same gene cluster, providing new tools for the transformation of triterpenoids and steroids.

Fusidic acid, helvolic acid and cephalosporin P<sub>1</sub> are the three representative fusidane-type antibiotics, and among them, only fusidic acid are clinically used. Since they have no cross resistance to commonly used antibiotics, chemical derivatization of fusidane-type antibiotics has been extensively carried out aiming at finding more potent analogues<sup>7–10</sup>. Unfortunately, derivatives with stronger activity than fusidic acid have not been found thus far. Combinational biosynthesis is an alternative approach to expand chemical diversity, which however requires a deep understanding of the biosynthesis of target compounds. Thus far, we have characterized the biosynthetic pathway for helvolic acid and fusidic acid, both of which share a six-enzyme catalyzed pathway at the early stage. This fact will provide clues to the identification of the gene cluster for cephalosporin P<sub>1</sub>. Notably, compared with the early-stage biosynthesis catalyzed by the six conserved enzymes in a strict reaction order, the post modification enzymes action independently without a strict order. This feature has driven us to use a combinational biosynthetic approach to expand the

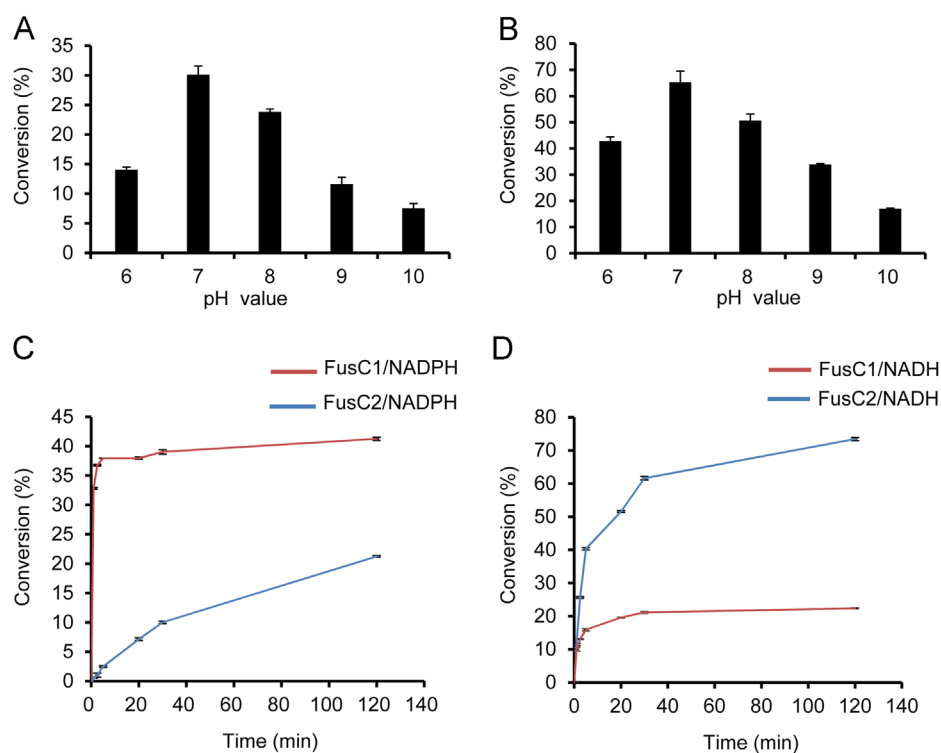


**Figure 4** Comparison of the catalytic property between FusC1 and FusC2. (A) Effects of the pH on the catalytic activity of FusC1. (B) Effects of the pH on the catalytic activity of FusC2. (C) Comparison of the catalytic efficiency of FusC1 and FusC2 in the presence of NADPH. (D) Comparison of the catalytic efficiency of FusC1 and FusC2 in the presence of NADH. All values are means  $\pm$  standard error from two experiments.

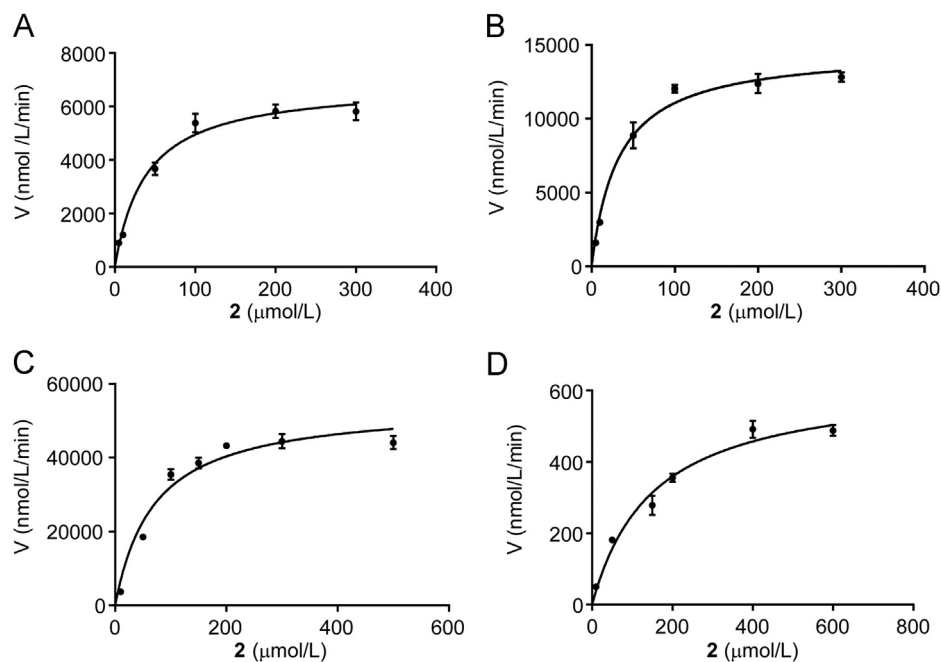


**Figure 5** Steady-state enzyme kinetics of FusC1 and FusC2 using **2** as a substrate. (A) Kinetic parameters for FusC1 were determined at a saturating concentration of NADH. (B) Kinetic parameters for FusC2 were determined at a saturating concentration of NADH. (C) Kinetic parameters for FusC1 were determined at a saturating concentration of NADPH. (D) Kinetic parameters for FusC2 were determined at a saturating concentration of NADPH.

chemical diversity by introduction of these post modification genes from different origins into the six-gene expression strain.

Hydroxylation at C-11 $\alpha$  position is important for the anti-bacterial activity of fusidic acid (Table 3), which is catalyzed by a cytochrome P450 monooxygenase FusB1. Thus far, only three

steroid 11 $\alpha$ -hydroxylases CYP509C12, CYP5311B1 and 11 $\alpha$ -SH<sup>Aoch</sup> from *Rhizopus oryzae*, *Aspergillus ochraceus* and *Absidia caerulea*, respectively, have been reported<sup>26–28</sup>. Phylogenetic analysis of FusB1 with other fungi-derived P450 enzymes involved triterpenoid/steroid modifications revealed that FusB1

**Table 2** Kinetic data for FusC1 and FusC2 using **2** as a substrate.

Condition	$K_m$ ( $\mu\text{mol/L}$ )	$V_{\text{max}}$ (nmol/L/min)	$K_{\text{cat}}$ (1/min)	$K_{\text{cat}}/K_m$ (L/min/ $\mu\text{mol}$ )
FusC1 ( <b>2</b> + NADH cofactor)	38.77 $\pm$ 7.75	6867 $\pm$ 363.30	34.34 $\pm$ 1.82	0.89
FusC2 ( <b>2</b> + NADH cofactor)	32.80 $\pm$ 5.96	14693 $\pm$ 667.50	73.47 $\pm$ 3.34	2.24
FusC1 ( <b>2</b> + NADPH cofactor)	70.03 $\pm$ 20.00	54484 $\pm$ 4501	272.42 $\pm$ 22.51	3.89
FusC2 ( <b>2</b> + NADPH cofactor)	151.20 $\pm$ 37.42	630.50 $\pm$ 55.29	3.15 $\pm$ 0.28	0.02

**Table 3** Anti-*Staphylococcus aureus* 209P activity of compounds.

Compound	MIC ( $\mu\text{g/mL}$ )
<b>1</b> (Fusidic acid)	0.004
<b>3</b>	0.25
<b>4</b>	8
<b>5</b>	0.25
Tobramycin	0.06

form a cluster with CYP5311B1 and  $11\alpha\text{-SH}^{\text{Aoch}}$ , but not with steroid  $11\alpha$ -hydroxylase CYP509C12, and CYP5150L8 involved in biosynthesis of ganoderic acid<sup>29</sup> and VidA/D/K for demethoxyviridin biosynthesis<sup>30</sup> (Supporting Information Fig. S5). Notably, FusB1 is far from the clade of HelB2/FusB2, HelB4/FusB3 and HelB1/FusB4, ruling out the possibility that FusB2 is generated from FusB1 by gene duplication. This newly identified FusB1 will be developed as a useful tool for  $11\alpha$ -hydroxylation of other steroids and triterpenoids.

Different from the biosynthetic gene cluster of helvolic acid that contains only one SDR gene, we have identified two SDR genes, *fusC1* and *fusC2*, from the *fus* cluster. FusC2, the homologue of HelC, catalyzes the dehydrogenation of  $3\beta\text{-OH}$  to trigger the oxidative decarboxylation, whereas FusC1 is for the specific reduction of 3-keto to  $3\alpha\text{-OH}$  during the biosynthesis of fusidic acid. We also found that FusC2 could specifically reduce the 3-keto to  $3\beta\text{-OH}$ , but this conversion is hardly detected in the presence of FusC1. Sequence comparison of FusC1 with FusC2 shows rather low sequence homology (26% identity). Phylogenetic analysis of FusC1 and FusC2 as well as other fungi-derived SDR enzymes showed that FusC1 belongs to the family of “extended (e)” SDRs, while FusC2 belongs to the family of “classical” SDRs, respectively (Supporting Information Fig. S6)<sup>31</sup>. The molecular basis for how FusC1 and FusC2 specifically convert the same substrate to epimers requires further X-ray crystallographic study.

Although both SDR enzymes could accept the 3-keto derivatives and reduce them into  $3\alpha\text{-OH}$  or  $3\beta\text{-OH}$  products, the efficiency of HelC or FusC2 seems much lower than that of FusC1 as we could not detect the  $3\beta\text{-OH}$  products when FusC1 was co-expressed in the six-gene expression strain. Comparison of the catalytic efficiency of FusC1 and FusC2 revealed that in the presence of NADPH, FusC1 is about 200-fold more active than FusC2, while in the presence of NADH, FusC1 is less active than FusC2. These facts raised a possibility that the predominant production of  $3\alpha\text{-OH}$  products is possibly caused by the larger amount of NADPH relative to NADH in the fungi. Even though, the possibility that the predominant production of  $3\alpha\text{-OH}$  products is caused by the larger amount of *fusC1* relative to *fusC2* in the fungi could not be ruled out.

## 5. Conclusions

In conclusion, using a combinational biosynthetic strategy, we have firstly identified the biosynthetic gene cluster of the clinically used drug fusidic acid and characterized its full biosynthetic pathway. The newly discovered two SDR enzymes could be useful tools for transformation of steroids and triterpenoids. Our study has set a stag to use biosynthetic approach to expand the chemical diversity of fusidane-type antibiotics.

## Acknowledgments

We thank Professor K. Gomi (Tohoku University) and Professor K. Kitamoto (The University of Tokyo) for the *Aspergillus oryzae* NSAR1 heterologous expression system. This work was mainly supported by grants from the National Natural Science Foundation of China (31870032, 3171101305, and 31670036); the 111 Project of Ministry of Education of the People's Republic of China (B13038); the JST/NSFC Strategic International Collaborative Research Program; Japanese-Chinese Collaborative Research Program; Chang Jiang Scholars Program (Hao Gao, 2017) from the Ministry of Education of China; Guangdong Special Support Program (2016TX03R280); Guangdong Province Universities and Colleges Pearl River Scholar Funded Scheme (Hao Gao, 2014); and K. C. Wong Education Foundation (Hao Gao, 2016); Guangzhou Science and Technology Project (201707010266, China); the Fundamental Research Funds for the Central Universities (21617495); Kobayashi International Scholarship Foundation; a Grant-in-Aid for Scientific Research from the Ministry of Education, Culture, Sports, Science and Technology, Japan (JSPS KAKENHI Grant Number JP15H01836 and JP16H06443).

## Appendix A. Supporting information

Supplementary data associated with this article can be found in the online version at <https://doi.org/10.1016/j.apsb.2018.10.007>.

## References

- Zhao M, Gödecke T, Gunn J, Duan JA, Che CT. Protostane and fusidane triterpenes: a mini-review. *Molecules* 2013;**18**:4054–80.
- Godtfredsen WO, Jahnsen S, Lorck H, Roholt K, Tybring L. Fusidic acid: a new antibiotic. *Nature* 1962;**193**:987.
- Jones RN, Mendes RE, Sader HS, Castanheira M. *In vitro* antimicrobial findings for fusidic acid tested against contemporary (2008–2009) Gram-positive organisms collected in the United States. *Clin Infect Dis* 2011;**52**:S477–86.
- Bodley JW, Zieve FJ, Lin L, Zieve ST. Formation of the ribosome-G factor-GDP complex in the presence of fusidic acid. *Biochem Biophys Res Commun* 1969;**37**:437–43.

5. Zhou J, Lancaster L, Donohue JP, Noller HF. Crystal structures of EF-G-ribosome complexes trapped in intermediate states of translocation. *Science* 2013;**340**:1236086.
6. Fernandes P. Fusidic acid: a bacterial elongation factor inhibitor for the oral treatment of acute and chronic *Staphylococcal* infections. *Cold Spring Harb Perspect Med* 2016;**6**:a025437.
7. Von Daehne W, Godtfredsen WO, Rasmussen PR. Structure–activity relationships in fusidic acid-type antibiotics. *Adv Appl Microbiol* 1979;**25**:95–146.
8. Dauben WG, Kessel CR, Kishi M, Somei M, Tada M, Guillerm D. A formal total synthesis of fusidic acid. *J Am Chem Soc* 1982;**104**:303–5.
9. Duvold T, Jørgensen A, Andersen NR, Henriksen AS, Sørensen MD, Björkling F. 17S,20S-methanofusidic acid, a new potent semi-synthetic fusidane antibiotic. *Bioorg Med Chem Lett* 2002;**12**:3569–72.
10. Duvold T, Sørensen MD, Björkling F, Henriksen AS, Rastrup-Andersen N. Synthesis and conformational analysis of fusidic acid side chain derivatives in relation to antibacterial activity. *J Med Chem* 2001;**44**:3125–31.
11. Mulheim LJ, Caspi E. Mechanism of squalene cyclization. The biosynthesis of fusidic acid. *J Biol Chem* 1971;**246**:2494–501.
12. Lodeiro S, Xiong Q, Wilson WK, Ivanova Y, Smith ML, May GS, et al. Protostadienol biosynthesis and metabolism in the pathogenic fungus *Aspergillus fumigatus*. *Org Lett* 2009;**11**:1241–4.
13. Mitsuguchi H, Seshime Y, Fujii I, Shibuya M, Ebizuka Y, Kushiro T. Biosynthesis of steroidal antibiotic fusidanes: functional analysis of oxidosqualene cyclase and subsequent tailoring enzymes from *Aspergillus fumigatus*. *J Am Chem Soc* 2009;**131**:6402–11.
14. Jin FJ, Maruyama J, Juvvadi PR, Arioka M, Kitamoto K. Development of a novel quadruple auxotrophic host transformation system by *argB* gene disruption using *adeA* gene and exploiting adenine auxotrophy in *Aspergillus oryzae*. *FEMS Microbiol Lett* 2004;**239**:79–85.
15. Lv JM, Hu D, Gao H, Kushiro T, Awakawa T, Chen GD, et al. Biosynthesis of helvolic acid and identification of an unusual C-4-demethylation process distinct from sterol biosynthesis. *Nat Commun* 2017;**8**:1644.
16. Zheng YM, Lin FL, Gao H, Zou G, Zhang JW, Wang GQ, et al. Development of a versatile and conventional technique for gene disruption in filamentous fungi based on CRISPR-Cas9 technology. *Sci Rep* 2017;**7**:9250.
17. Koyama N, Tokura Y, Takahashi Y, Tomoda H. New cyclodans B and C, potentiators of imipenem activity against methicillin-resistant *Staphylococcus aureus* produced by *Streptomyces* sp. K04-0144. *Acta Pharm Sin B* 2011;**1**:236–9.
18. Wang CX, Ding R, Jiang ST, Tang JS, Hu D, Chen GD, et al. Aldgamycins J–O, 16-membered macrolides with a branched octose unit from *Streptomyces* sp. and their antibacterial activities. *J Nat Prod* 2016;**79**:2446–54.
19. Dai P, Wang CX, Gao H, Wang QZ, Tang XL, Chen GD, et al. Characterization of methyltransferase AlmCII in chalcone biosynthesis: the first TylF family O-methyltransferase works on a 4'-deoxysugar. *ChemBiochem* 2017;**18**:1510–7.
20. Rastrup-Andersen N, Duvold T. Reassignment of the <sup>1</sup>H NMR spectrum of fusidic acid and total assignment of <sup>1</sup>H and <sup>13</sup>C NMR spectra of some selected fusidane derivatives. *Magn Reson Chem* 2002;**40**:471–3.
21. Godtfredsen WO, Rastrup-Andersen N, Vangedal S, Ollis WD. Metabolites of *Fusidium coccineum*. *Tetrahedron* 1979;**35**:2419–31.
22. Larsen KL, Andersen SB, Mørkbak AL, Wimmer R. Inclusion complexes of fusidic acid and three structurally related compounds with cyclodextrins. *J Incl Phenom Macrocycl Chem* 2007;**57**:185–90.
23. Matsuda Y, Quan Z, Mitsunashi T, Li C, Abe I. Cytochrome P450 for citreohydroin synthesis: oxidative derivatization of the andrastin scaffold. *Org Lett* 2016;**18**:296–9.
24. Matsuda Y, Iwabuchi T, Fujimoto T, Awakawa T, Nakashima Y, Mori T, et al. Discovery of key dioxygenases that diverged the paraherquonin and acetoxydehydroaustin pathways in *Penicillium brasilianum*. *J Am Chem Soc* 2016;**138**:12671–7.
25. Benach J, Filling C, Oppermann UC, Roversi P, Bricogne G, Berndt KD, et al. Structure of bacterial 3 $\beta$ /17 $\beta$ -hydroxysteroid dehydrogenase at 1.2 Å resolution: a model for multiple steroid recognition. *Biochemistry* 2002;**41**:14659–68.
26. Hull CM, Warrilow AGS, Rolley NJ, Price CL, Donnison IS, Kelly DE, et al. Co-production of 11 $\alpha$ -hydroxyprogesterone and ethanol using recombinant yeast expressing fungal steroid hydroxylases. *Biotechnol Biofuels* 2017;**10**:226.
27. Petrič Š, Hakki T, Bernhardt R, Žigon D, Črešnar B. Discovery of a steroid 11 $\alpha$ -hydroxylase from *Rhizopus oryzae* and its biotechnological application. *J Biotechnol* 2010;**150**:428–37.
28. Wang R, Sui P, Hou X, Cao T, Jia L, Lu F, et al. Cloning and identification of a novel steroid 11 $\alpha$ -hydroxylase gene from *Absidia coerulea*. *J Steroid Biochem Mol Biol* 2017;**171**:254–61.
29. Wang WF, Xiao H, Zhong JJ. Biosynthesis of a ganoderic acid in *Saccharomyces cerevisiae* by expressing a cytochrome P450 gene from *Ganoderma lucidum*. *Biotechnol Bioeng* 2018;**115**:1842–54.
30. Wang GQ, Chen GD, Qin SY, Hu D, Awakawa T, Li SY, et al. Biosynthetic pathway for furanosteroid demethoxyviridin and identification of an unusual pregnane side-chain cleavage. *Nat Commun* 2018;**9**:1838.
31. Hoffmann F, Maser E. Carbonyl reductases and pluripotent hydroxysteroid dehydrogenases of the short-chain dehydrogenase/reductase superfamily. *Drug Metab Rev* 2007;**39**:87–144.